Supplementary information to: Drivers of early diagenesis in sediments surrounding offshore wind foundations; a coupled data-modelling approach.

Emil De Borger[1,2], Karline Soetaert[1], Esther Cepeda Gamella[2, 3, 4], Arthur Capet[3, 5], Jan Vanaverbeke [2,3], Ulrike Braeckman[2, 3]

[1] Royal Netherlands Institute of Sea Research (NIOZ), Estuarine and Delta Systems, Korringaweg 7, Yerseke 4401NT, The Netherlands

[2] Ghent University, Marine Biology research group, Building S8 - De Sterre, Krijgslaan 297, 9000 Ghent, Belgium

[3]Royal Belgian Institute of Natural Sciences, Operational Directorate Natural Environment, Marine Ecology and Management, Vautierstraat 29, Brussels 1000, Belgium

[4]Ghent University, Isotope Bioscience laboratory – ISOFYS, Department of green Chemistry and Technology, Coupure links 653, Ghent 9000, Belgium

[5]Université Libre de Bruxelles, Biogeochemistry and modelling of the Earth System, Campus du Solbosch, Avenue F.F. Roosevelt 50, Brussels 1050, Belgium

Correspondence to: Emil De Borger (emil.de.borger@nioz.nl)

S1. Supplementary materials and methods

S1.1. Parametrization and rate equations of diagenetic model

The following equations outlined in Soetaert et al. (1996) describe mineralization process rates of the PermeableDia model, with parameter explanations in Table S. 3.

$$OxicMin_i = R_{Miner,i} \frac{O_2}{O_2 + Ks_{O2}^{oxic}} * TOC_i * \frac{1}{\Sigma lim} \quad \text{eq. S. 1}$$

$$Denit_i = R_{Miner,i} * \frac{NO_3}{NO_3 + Ks_{NO3}^{Denit}} * \left(1 - \frac{O_2}{O_2 + Kin_{O2}^{Denit}}\right) * TOC_i * \frac{1}{\Sigma lim} \quad \text{eq. S. 2}$$

$$AnoxMin_i = R_{Miner,i} * \left(1 - \frac{NO_3}{NO_3 + K_{NO3}^{AnoxMin}}\right) * \left(1 - \frac{O_2}{O_2 + Kin_{O2}^{AnoxMin}}\right) * TOC_i * \frac{1}{\Sigma lim} \quad \text{eq. S. 3}$$

For i = Fast and Slow (either the fast, or slow degrading organic matter pool).

$$\Sigma Lim = \frac{O_2}{O_2 + Ks_{O2}} + \frac{NO_3}{NO_3 + Ks_{NO3}} * \left(1 - \frac{O_2}{O_2 + Kin_{O2}^{Denit}}\right) + \left(1 - \frac{NO_3}{NO_3 + Kin_{NO3}^{AnoxMin}}\right) * \left(1 - \frac{O_2}{O_2 + Kin_{O2}^{AnoxMin}}\right) \quad \text{eq. S. 4}$$

$$SolidODU = R_{solid} * (AnoxMin_1 + AnoxMin_2) * \gamma_{TOC}^{ODU} * \frac{1-\phi}{\phi} \quad \text{eq. S. 5}$$

$$ODUoxid = R_{ODUox} * ODU * \frac{O_2}{O_2 + Ks_{ODUox}^{O2}} \quad \text{eq. S. 6}$$

$$NH_3oxid = R_{Nitrif} * NH_3 * \frac{O_2}{O_2 + Ks_{Nitrif}^{O2}} - [OxicMin_1 + \gamma_{TOC1}^{N} * OxicMin_2 + \gamma_{TOC2}^{N}] * \frac{(1-\phi)}{\phi} \quad \text{eq. S. 7}$$

From which follow the rates of change (where @ denotes all transport processes):

$$\frac{dTOC_i}{dt} = @ - OxicMin_i - Denit_i - AnoxMin_i \quad (= @ - R_{Miner,i} * TOC_i) \quad \text{eq. S. 8}$$

$$\frac{dODU}{dt} = @ + (AnoxMin_1 + AnoxMin_2) * \gamma_{TOC}^{ODU} * \frac{1-\phi}{\phi} - ODU_{oxid} - SolidODU \qquad \textit{eq. S. 9}$$

$$\frac{dO_2}{dt} = @ - (OxicMin_1 + OxicMin_2) * \gamma_{TOC}^{O2} * \frac{1-\phi}{\phi} - ODU_{oxid} - NH_3oxid * \gamma_{NH3}^{O2} \qquad \textit{eq. S. 10}$$

$$\frac{dNO_3}{dt} = @ - (Denit_1 + Denit_2) * \gamma_{TOC}^{NO3} * \frac{1-\phi}{\phi} + NH_3oxid \qquad \textit{eq. S. 11}$$

$$\frac{dNH_3}{dt} = @ + \frac{[OxicMin_1 * Denit_1 + AnoxMin_1] * \gamma_{TOC1}^{N} - [OxicMin_2 + Denit_2 + AnoxMin_2] * \gamma_{TOC2}^{N}}{1 + NH_3ads} * \frac{1-\phi}{\phi} * \frac{NH_3oxid}{1 + NH_3ads} \qquad \textit{eq. S. 12}$$

S1.2. Bioturbation – reactivity – bioturbation depth

Bioturbation depth (*L*) was calculated from the bioturbation coefficient *Db* and the organic matter reactivity (*k*) using the formula provided in Middelburg et al., 2019 (*eq. S. 13*):

$$L = 4.6\sqrt{\frac{D_b}{k}} \qquad \textit{eq. S.13}$$

where *k* is calculated from reaction rates for fast and slow degrading fractions (*rFast*, rSlow) and the proportions of those fractions (*pFast*, 1 – *pFast* respectively).

S2. Supplementary figures

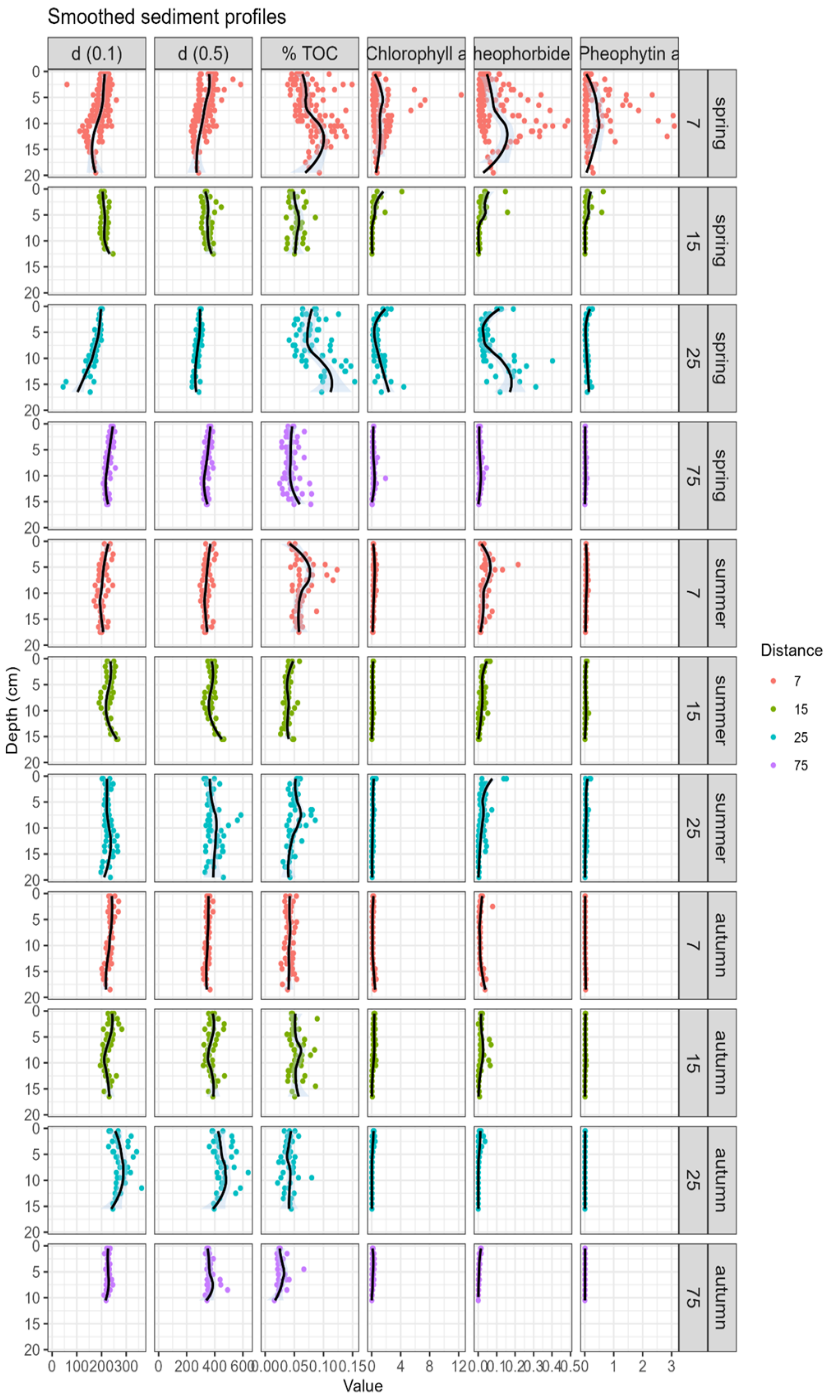

Figure S. 1: Measurements (points) of fine sediment fraction (d0.1), median grain size (d0.5), total organic carbon (TOC, %), chlorophyll a (Chl a, µg g^{-1}), pheophorbide a (µg g^{-1}), and pheophytin a (µg g^{-1}) for the different season – distance from SPL combinations. Averaged, smoothed profiles shown by black line.

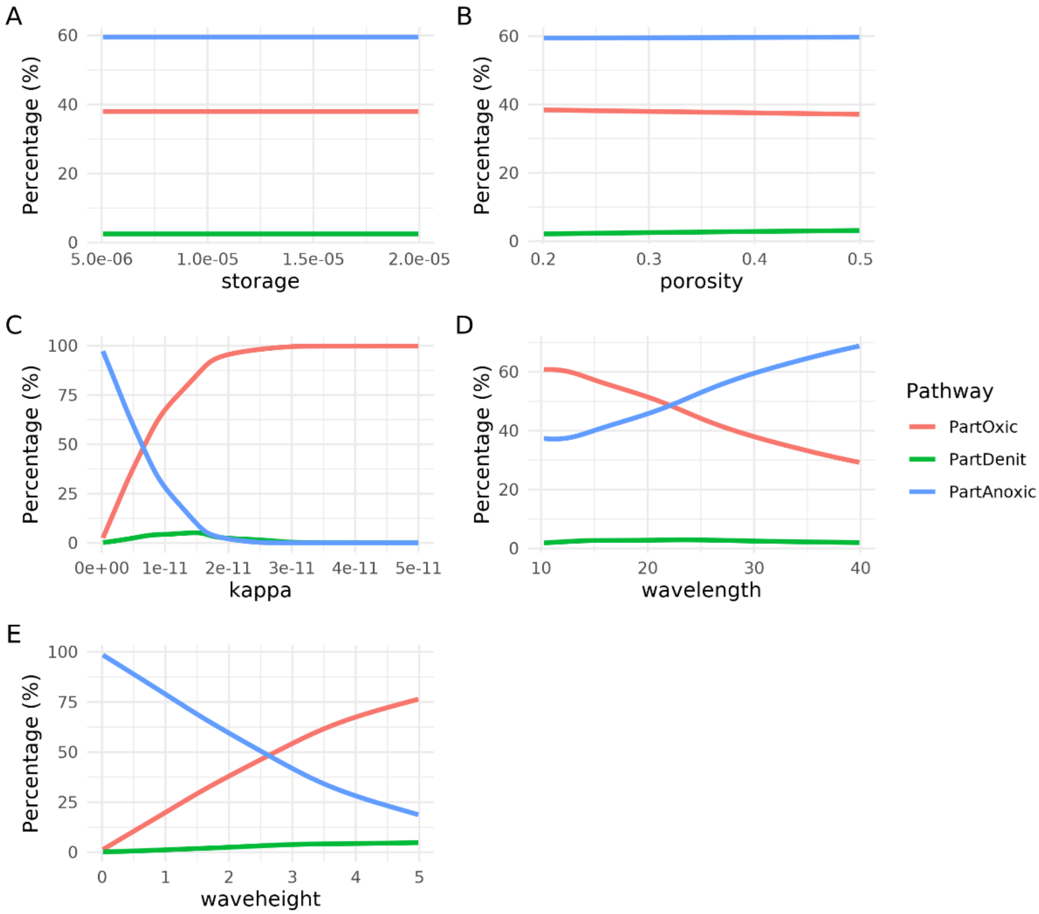

Figure S. 2: Response of division of total mineralization to (grouped) mineralization processes (y-axis, in %) to variations in (A) storage (m^{-1}), (B) porosity, (C) kappa-permeability (m^{2}), (D) ripple length of bedform (cm), and (E) ripple height of bedform (cm), while keeping all other parameter values fixed.

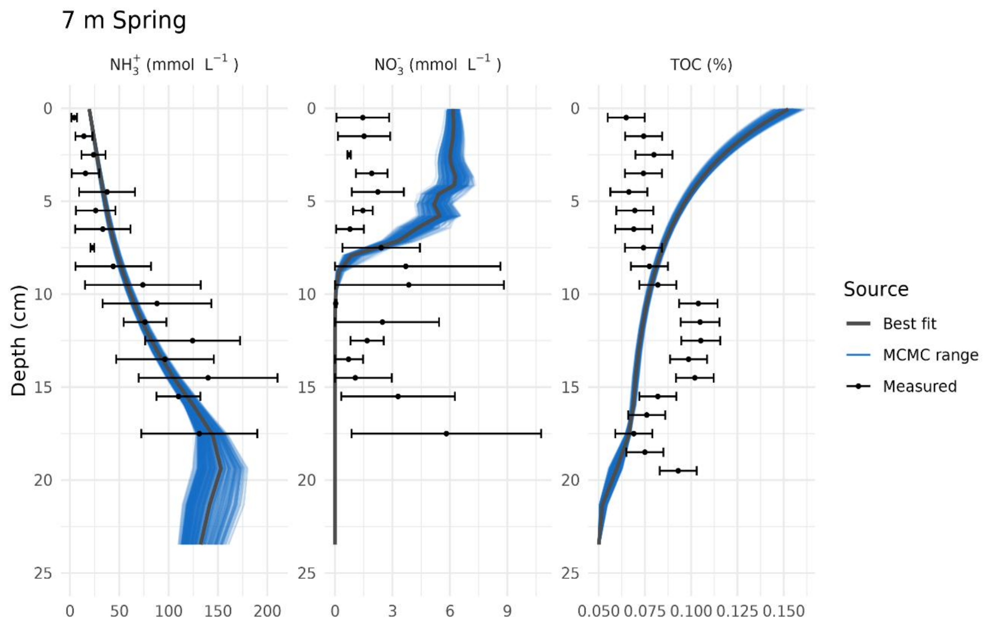

Figure S. 3: Modelled profiles (black line = best fit, blue lines = additional MCMC accepted fits), and average measured concentrations with standard deviations (black dots and error bars) for the 7 m – spring samples, for ammonia (NH_3), nitrate (NO_3^-), and TOC.

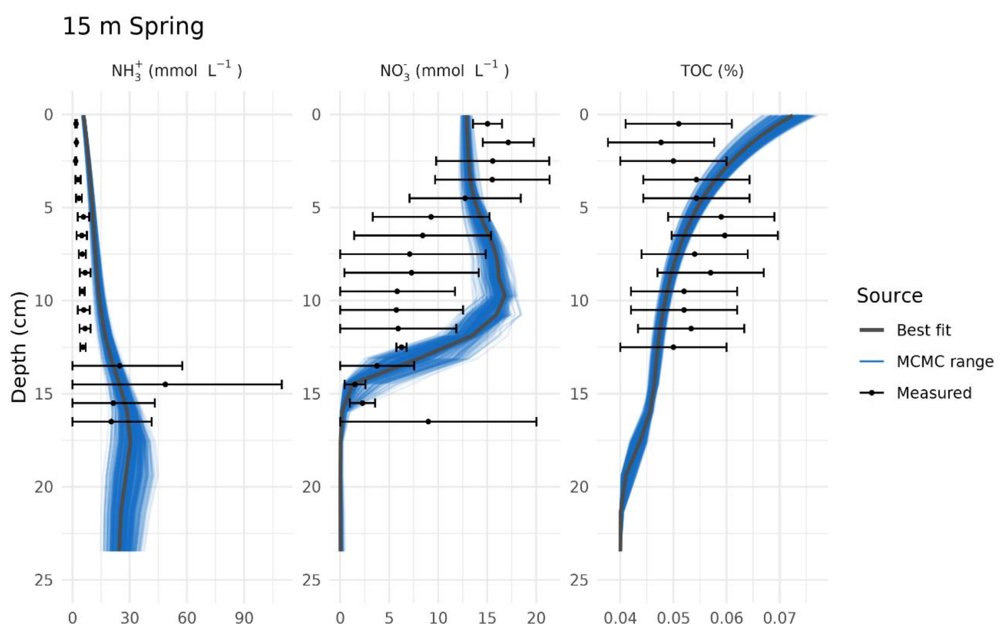

Figure S. 4: Modelled profiles (black line = best fit, blue lines = additional MCMC accepted fits), and average measured concentrations with standard deviations (black dots and error bars) for the 15 m – spring samples, for ammonia (NH_3), nitrate (NO_3^-), and TOC.

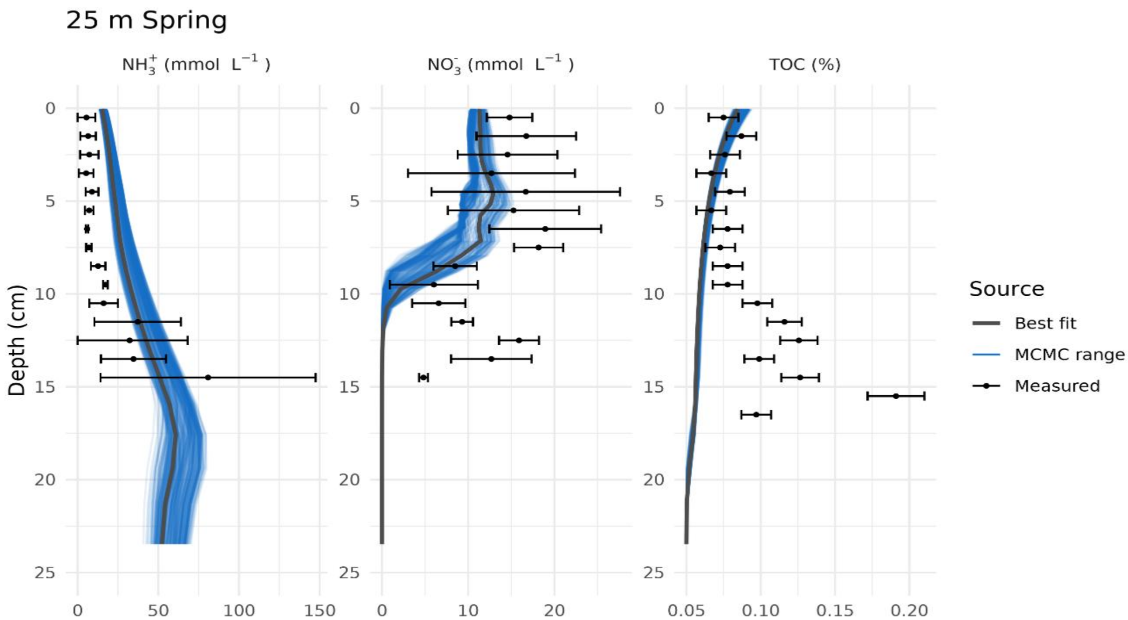

Figure S. 5: Modelled profiles (black line = best fit, blue lines = additional MCMC accepted fits), and average measured concentrations with standard deviations (black dots and error bars) for the 25 m – spring samples, for ammonia (NH_3), nitrate (NO_3^-), and TOC.

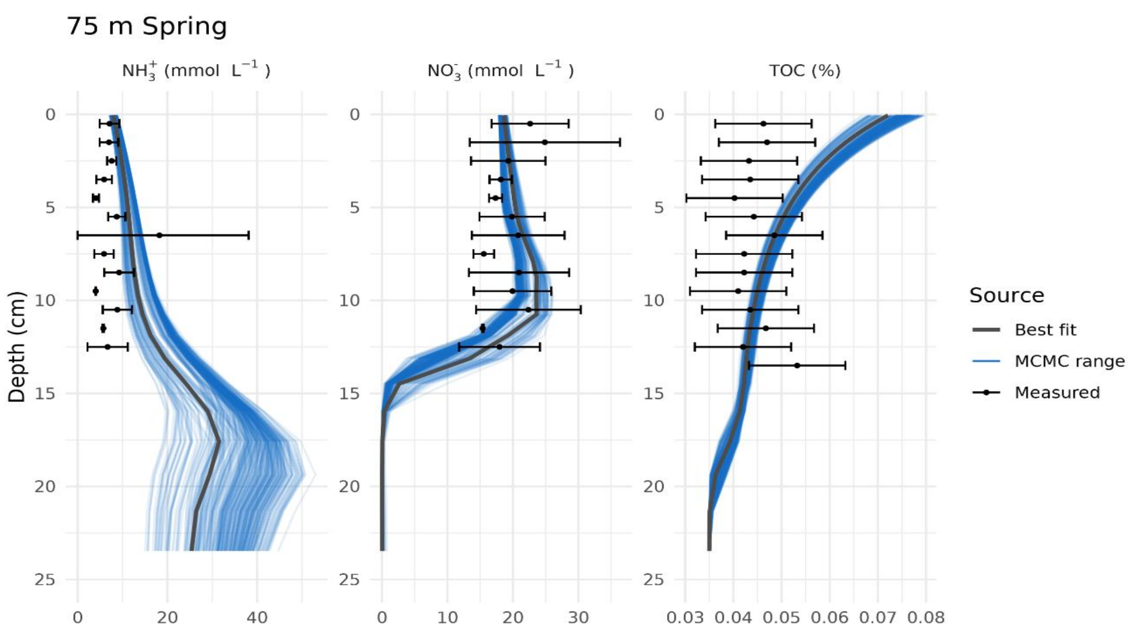

Figure S. 6: Modelled profiles (black line = best fit, blue lines = additional MCMC accepted fits), and average measured concentrations with standard deviations (black dots and error bars) for the 75 m – spring samples, for ammonia (NH_3), nitrate (NO_3^-), and TOC.

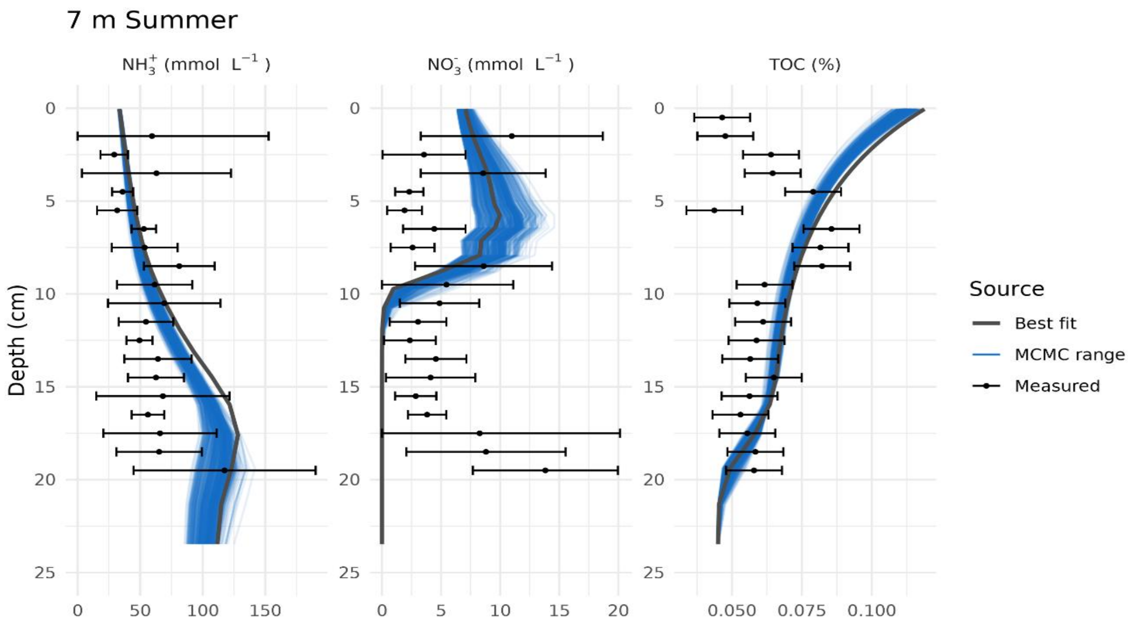

Figure S. 7: Modelled profiles (black line = best fit, blue lines = additional MCMC accepted fits), and average measured concentrations with standard deviations (black dots and error bars) for the 7 m – summer samples, for ammonia (NH_3), nitrate (NO_3^-), and TOC.

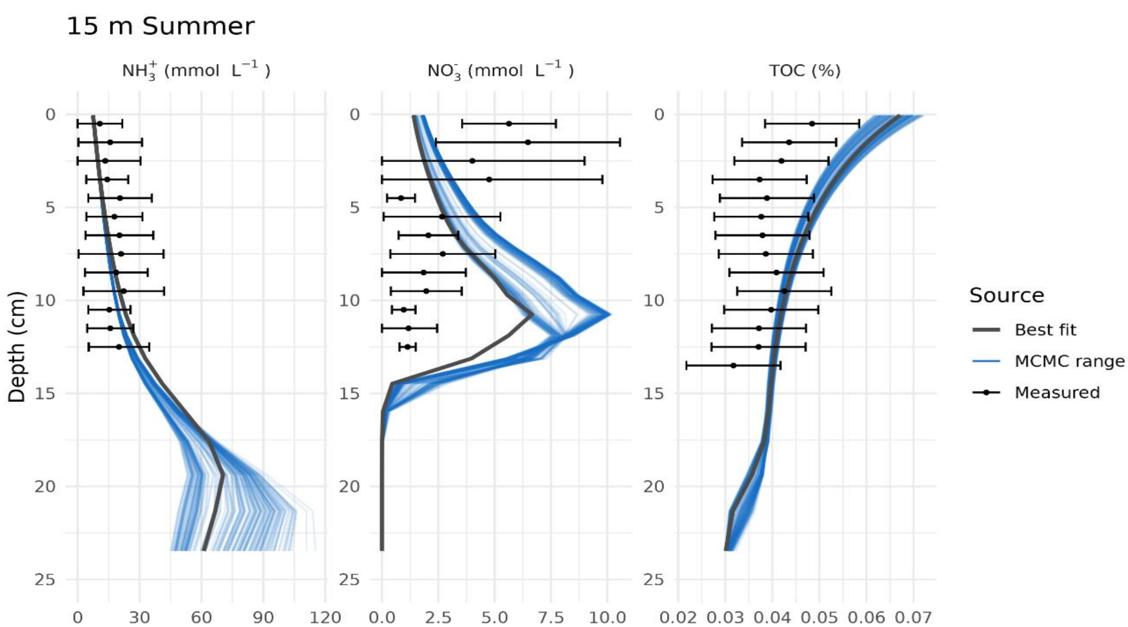

Figure S. 8: Modelled profiles (black line = best fit, blue lines = additional MCMC accepted fits), and average measured concentrations with standard deviations (black dots and error bars) for the 15 m – summer samples, for ammonia (NH_3), nitrate (NO_3^-), and TOC.

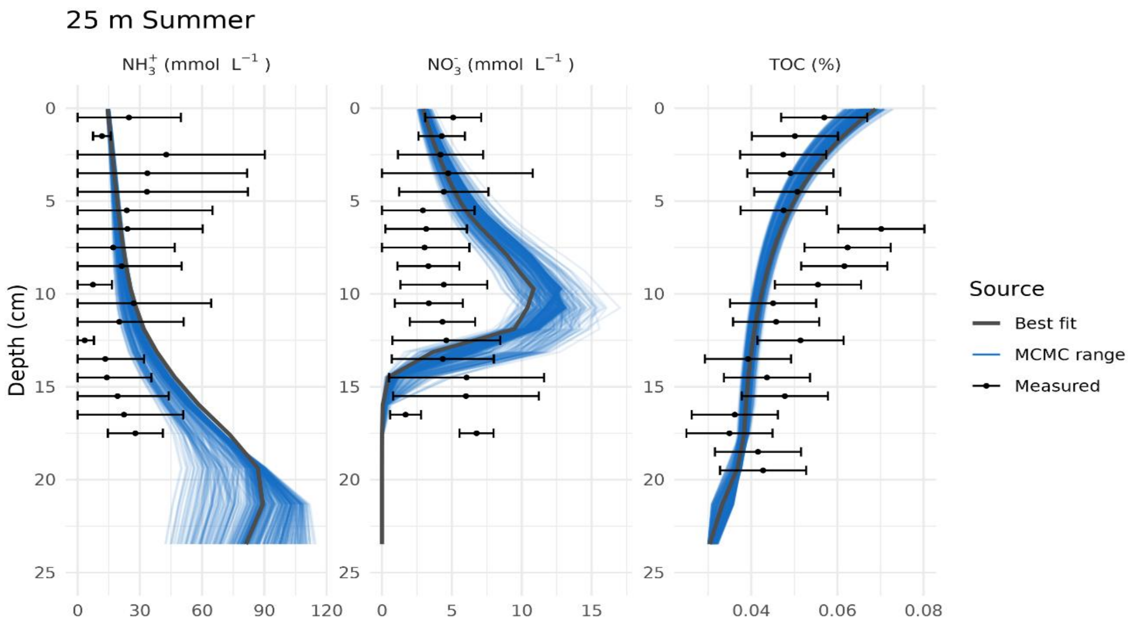

Figure S. 9: Modelled profiles (black line = best fit, blue lines = additional MCMC accepted fits), and average measured concentrations with standard deviations (black dots and error bars) for the 25 m – summer samples, for ammonia (NH_3), nitrate (NO_3^-), and TOC.

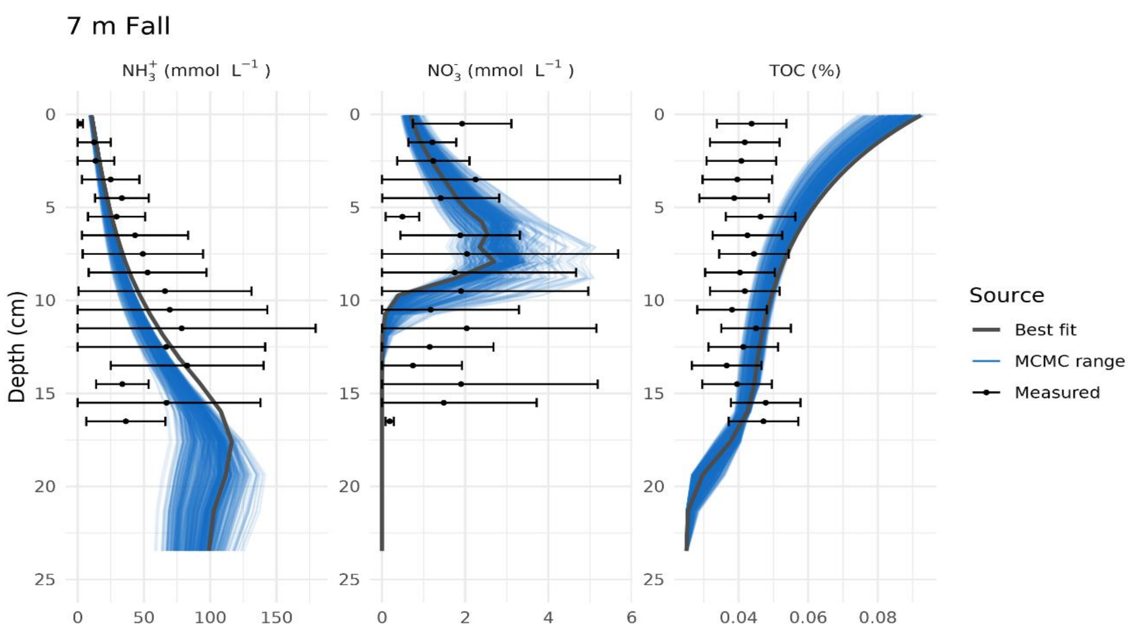

Figure S. 10: Modelled profiles (black line = best fit, blue lines = additional MCMC accepted fits), and average measured concentrations with standard deviations (black dots and error bars) for the 7 m – fall samples, for ammonia (NH_3), nitrate (NO_3^-), and TOC.

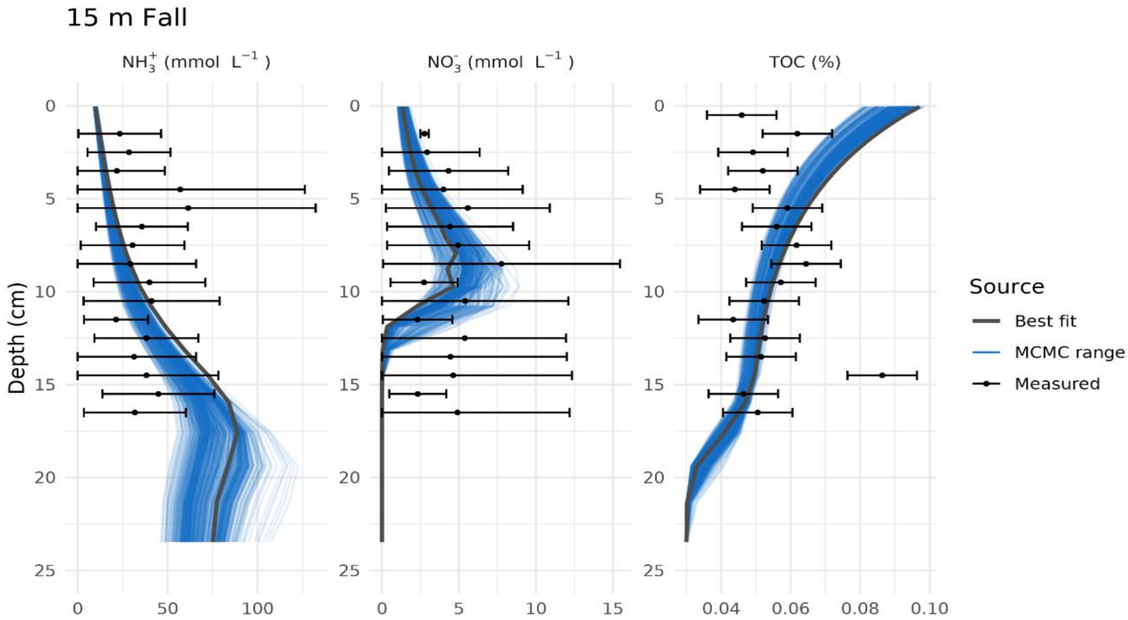

Figure S. 11: Modelled profiles (black line = best fit, blue lines = additional MCMC accepted fits), and average measured concentrations with standard deviations (black dots and error bars) for the 15 m – fall samples, for ammonia (NH_3), nitrate (NO_3^-), and TOC.

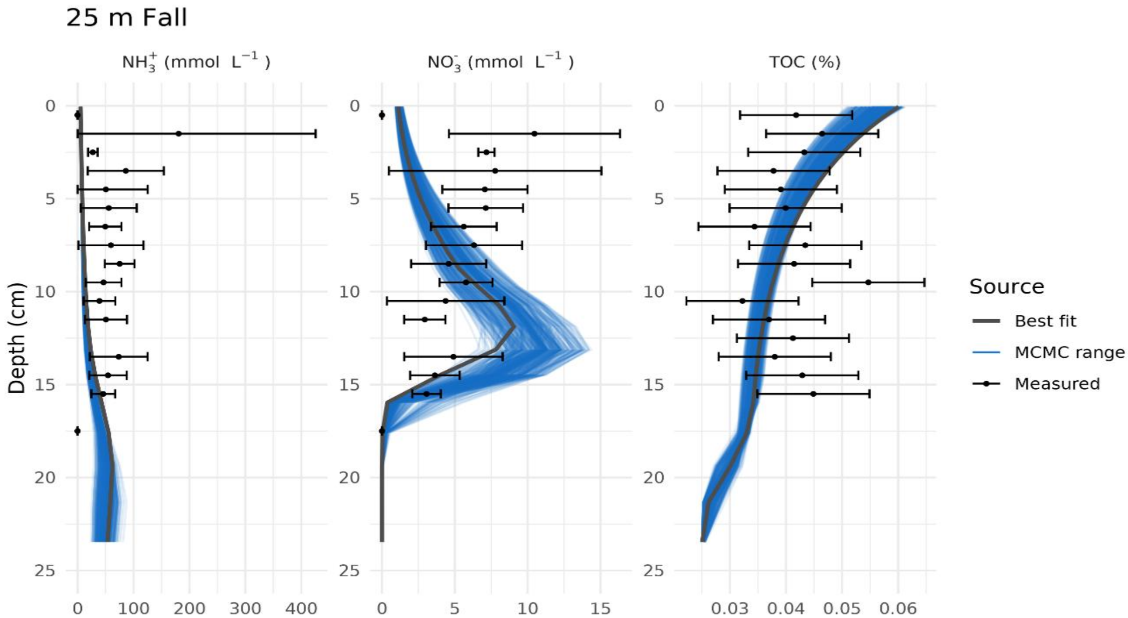

Figure S. 12: Modelled profiles (black line = best fit, blue lines = additional MCMC accepted fits), and average measured concentrations with standard deviations (black dots and error bars) for the 25 m – fall samples, for ammonia (NH_3), nitrate (NO_3^-), and TOC.

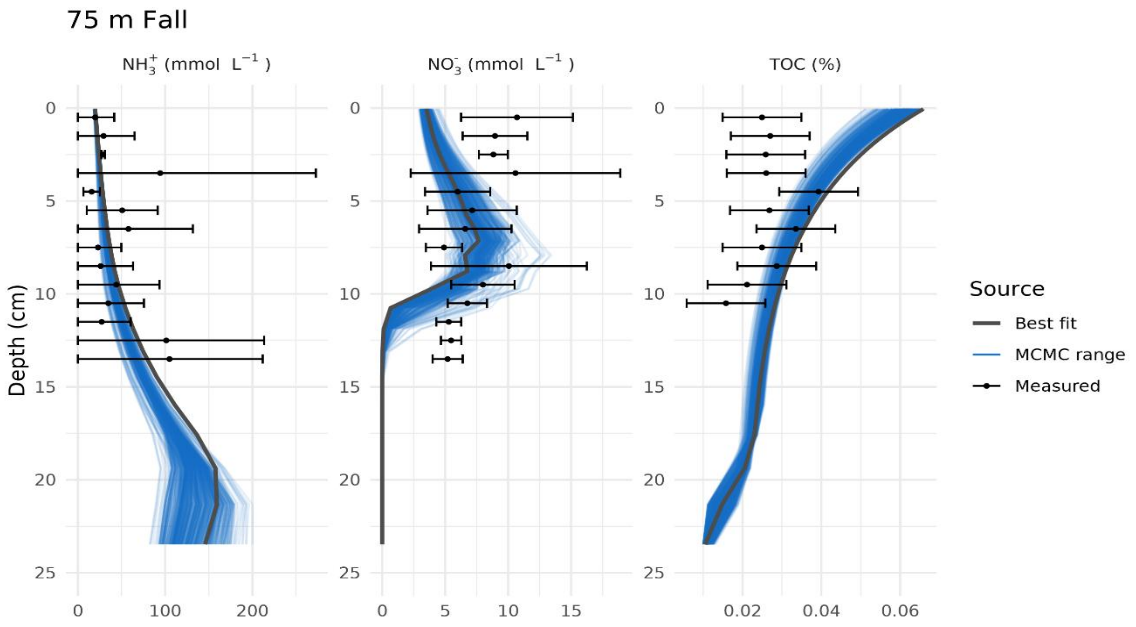

Figure S. 13: Modelled profiles (black line = best fit, blue lines = additional MCMC accepted fits), and average measured concentrations with standard deviations (black dots and error bars) for the 75 m – fall samples, for ammonia (NH_3), nitrate (NO_3^-), and TOC.

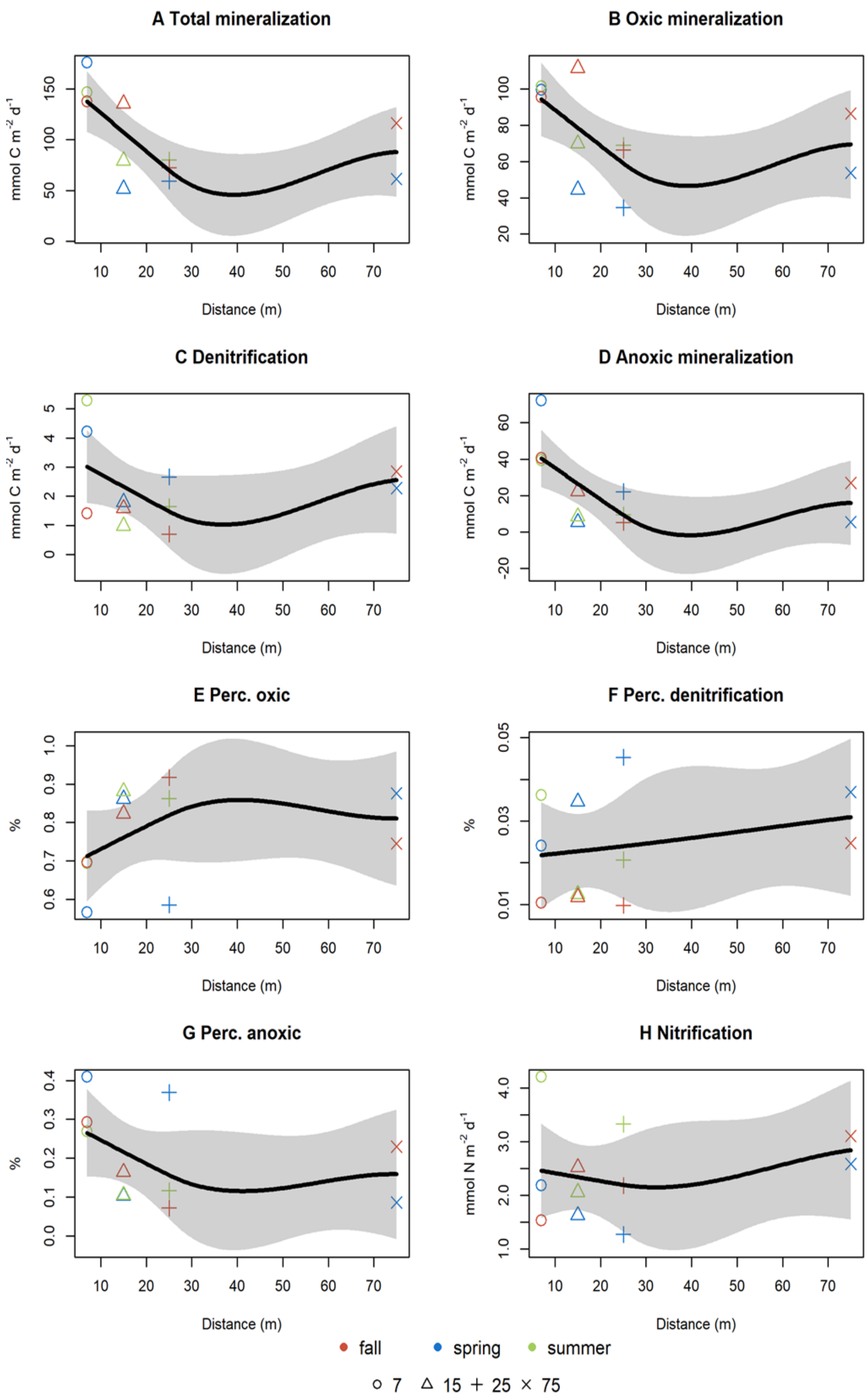

Figure S. 14: Model outputs (y-axis) over distance from the SPL (x-axis). Dots show model output, coloured per season, and a different shape per distance from the SPM (legend). Black line shows loess smoother, and its 95 % confidence interval (gray band).

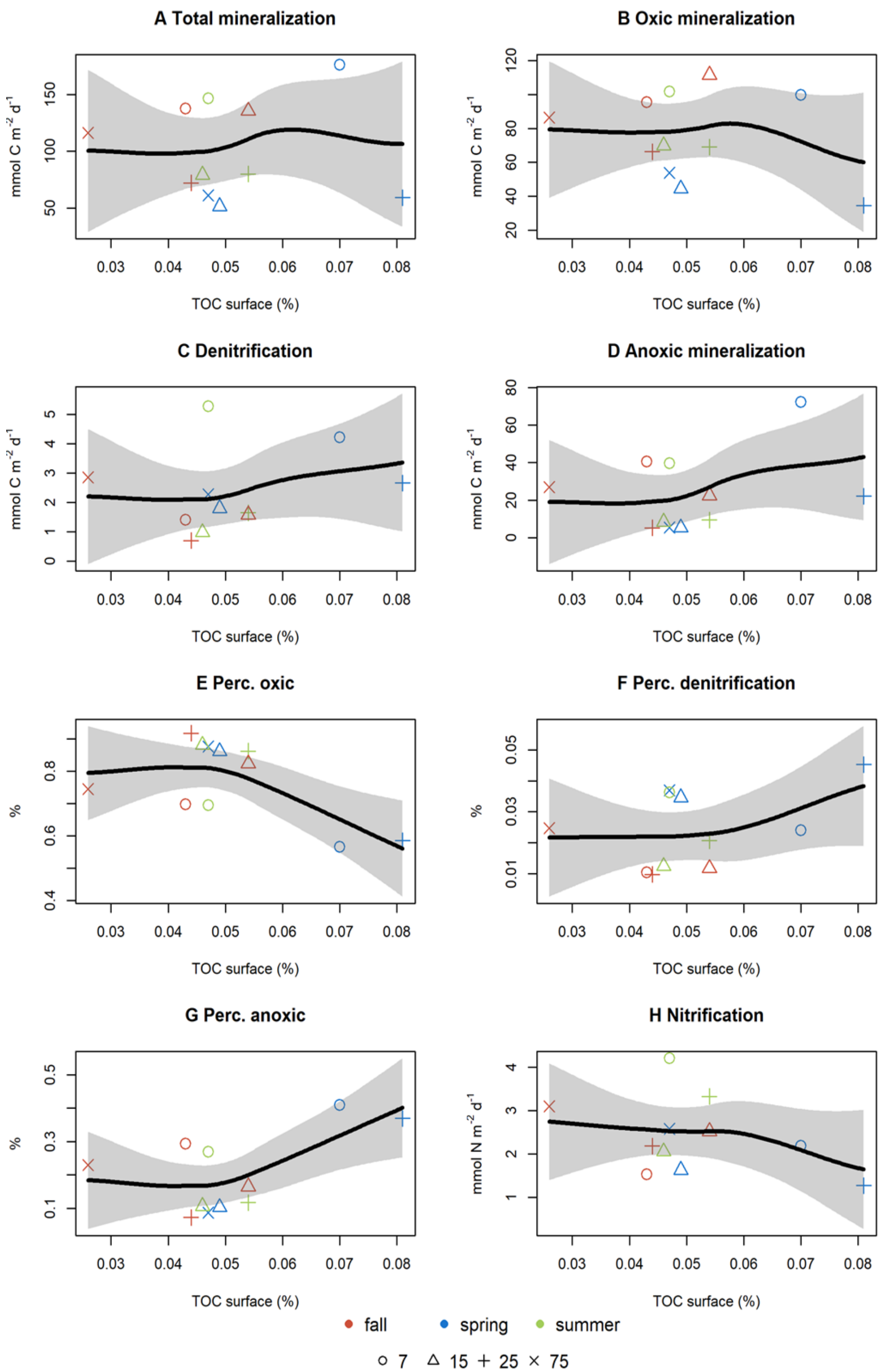

Figure S. 15: Model outputs (y-axis) over surface TOC content (x-axis). Dots show model output, coloured per season, and a different shape per distance from the SPM (legend). Black line shows loess smoother, and its 95 % confidence interval (gray band).

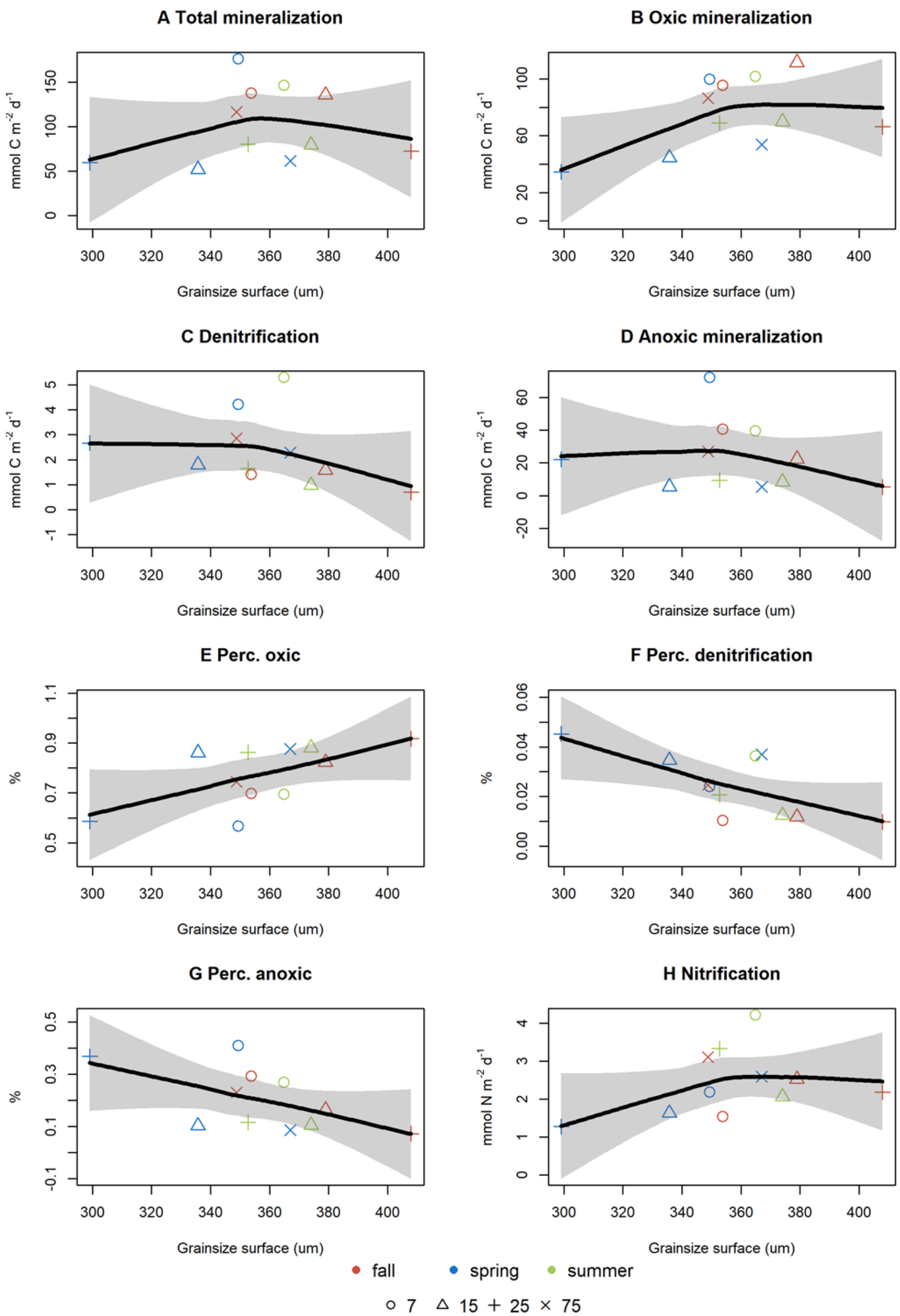

Figure S. 16: Model outputs (y-axis) over median grain size (x-axis). Dots show model output, coloured per season, and a different shape per distance from the SPM (legend). Black line shows loess smoother, and its 95 % confidence interval (gray band).

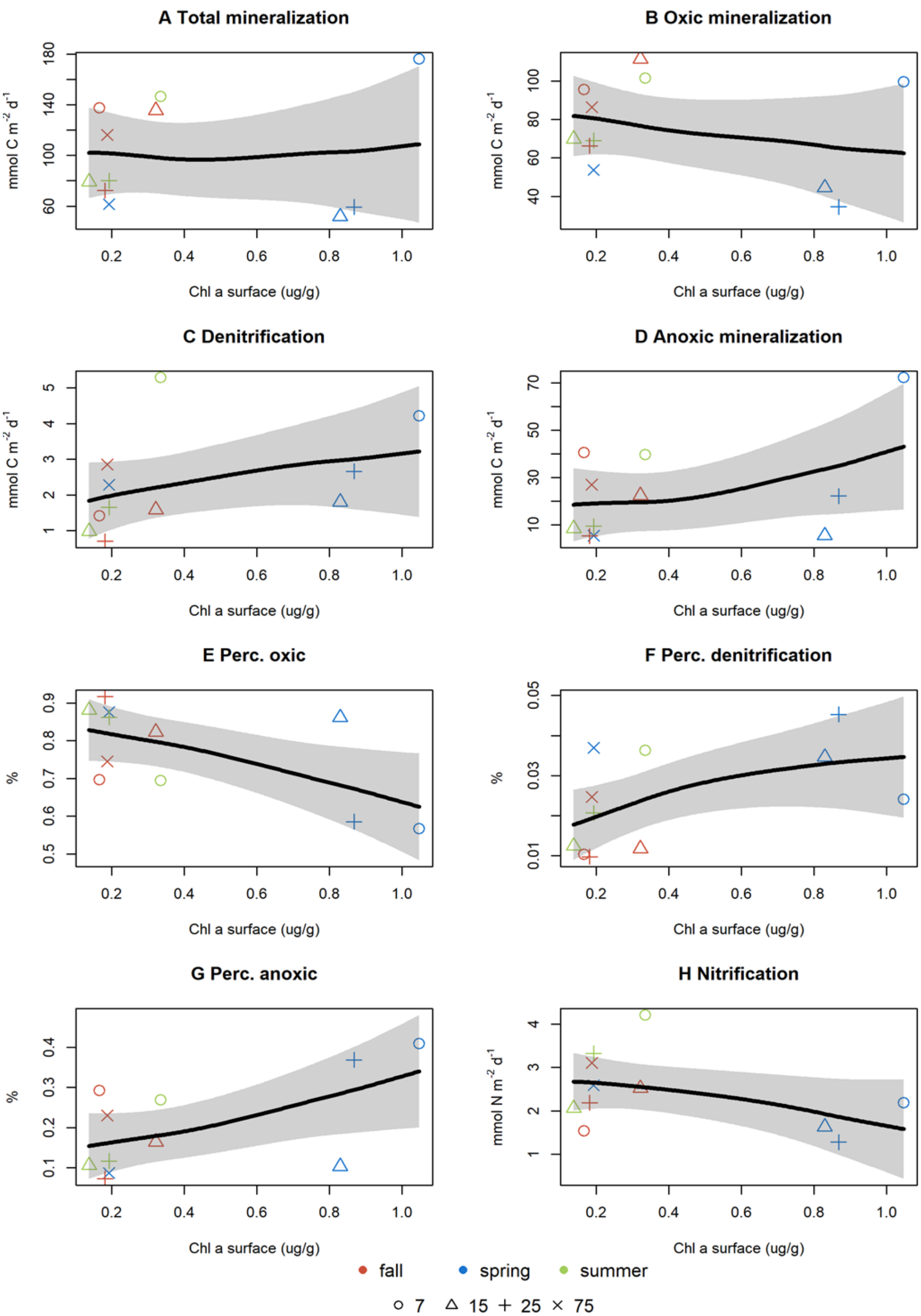

Figure S. 17: Model outputs (y-axis) over surface chlorophyll a content (x-axis). Dots show model output, coloured per season, and a different shape per distance from the SPM (legend). Black line shows loess smoother, and its 95 % confidence interval (gray band).

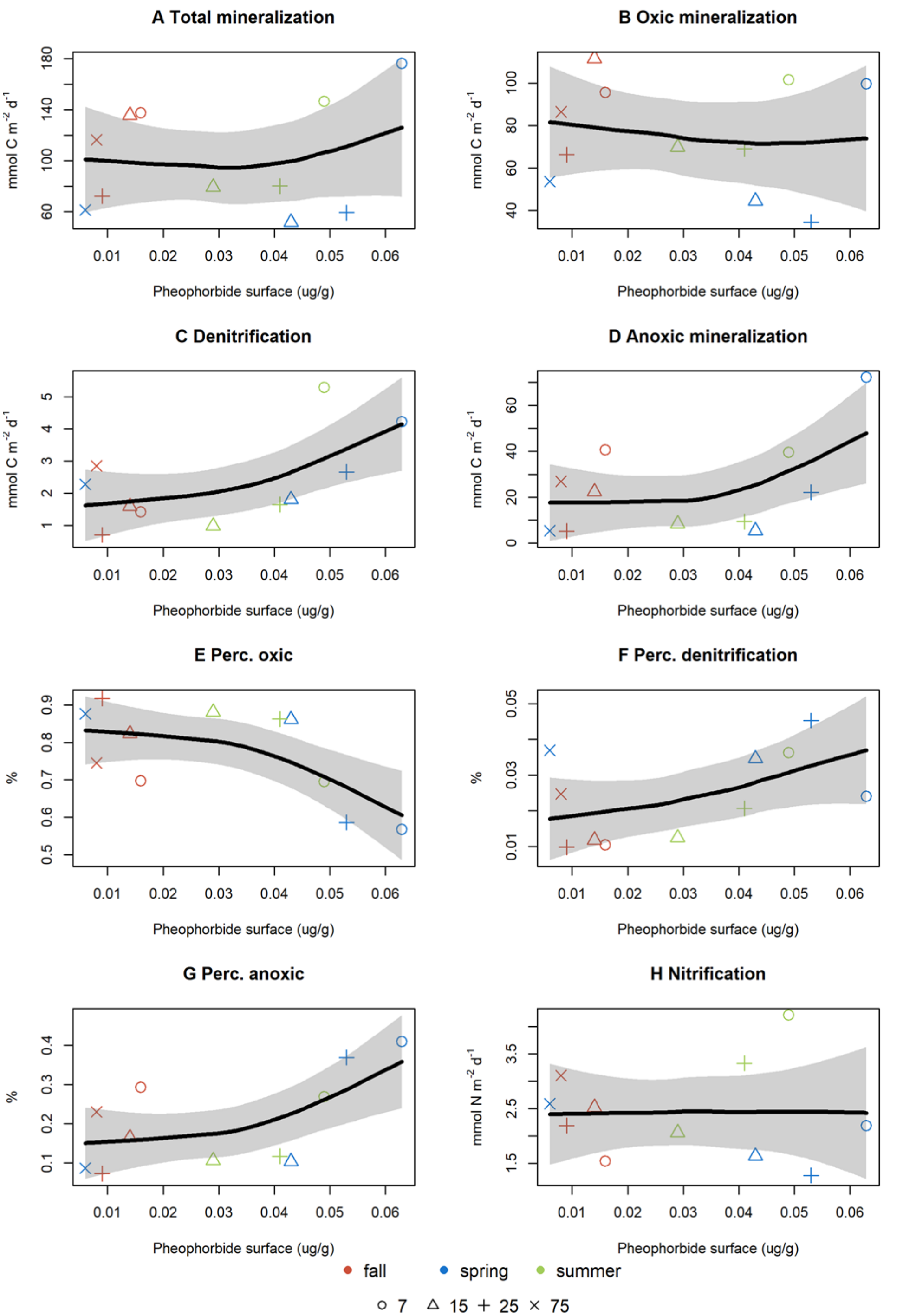

Figure S. 18: Model outputs (y-axis) over pheophorbide content (x-axis). Dots show model output, coloured per season, and a different shape per distance from the SPM (legend). Black line shows loess smoother, and its 95 % confidence interval (gray band).

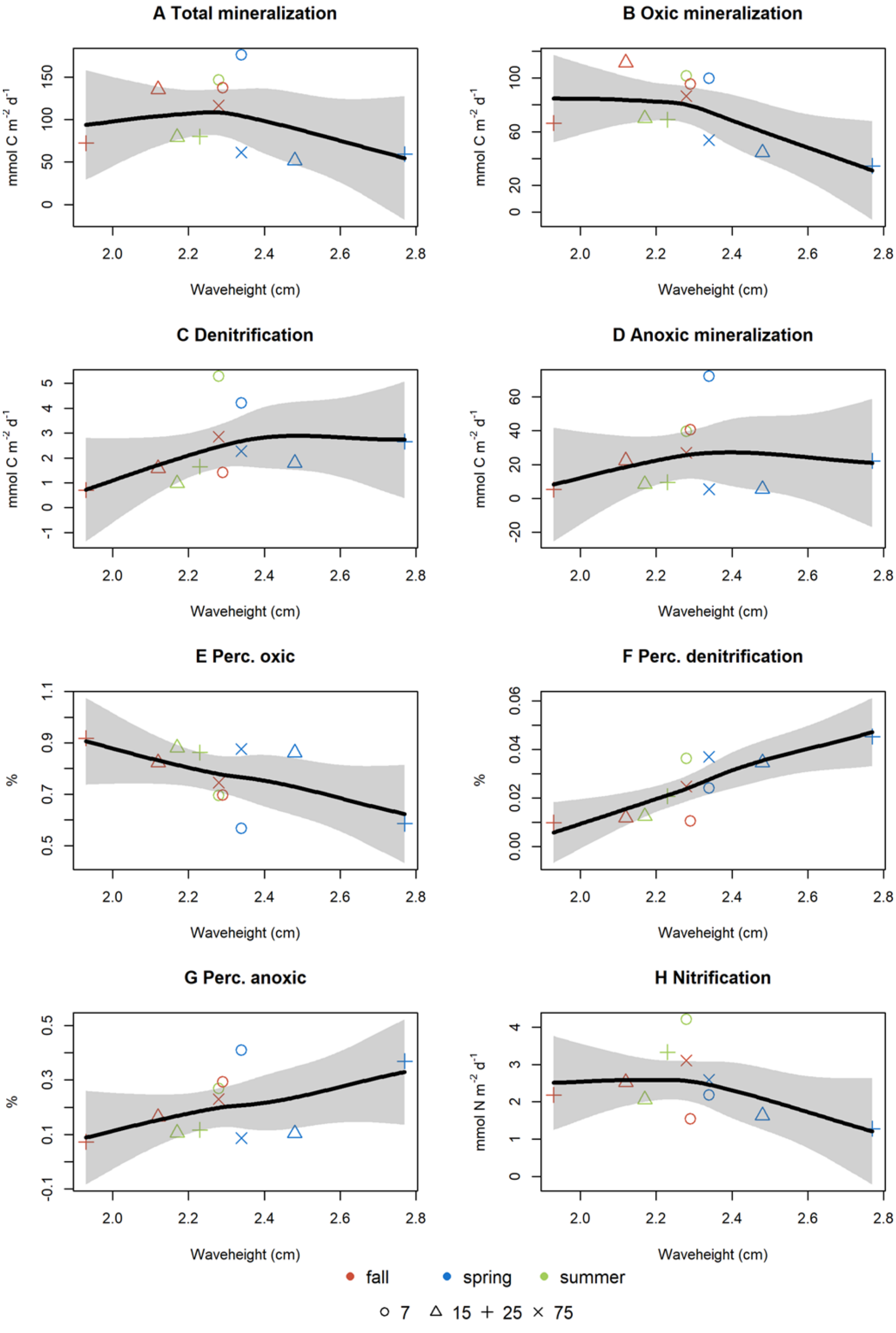

Figure S. 19: Model outputs (y-axis) over ripple height (x-axis). Dots show model output, coloured per season, and a different shape per distance from the SPM (legend). Black line shows loess smoother, and its 95 % confidence interval (gray band).

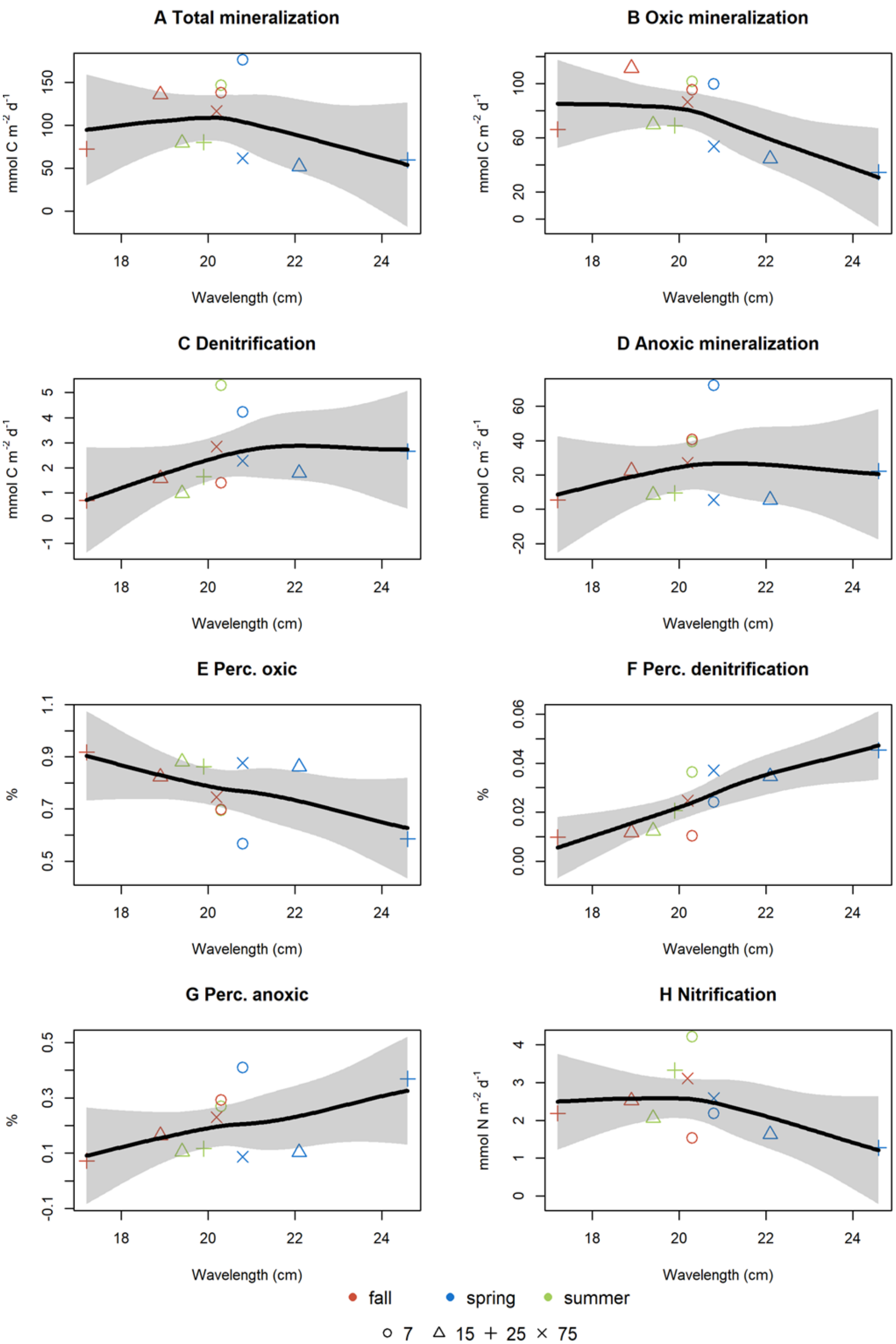

Figure S. 20: Model outputs (y-axis) over ripple length (x-axis). Dots show model output, coloured per season, and a different shape per distance from the SPM (legend). Black line shows loess smoother, and its 95 % confidence interval (gray band).

S3. Supplementary tables

Table S. 1: Details of sample collection.

Season	Distance SPL (m)	Sampling date	Sample type	Bottom water temperature	Salinity	Campaign code
Spring	7	27/04/2022	Scientific diver	9.9	32.6	SiSt_22-220
	15	29/03/2022	Scientific diver	8.25	33.4	BE2022_08
	25	28/03/2022	Scientific diver	8.25	33.4	BE2022_08
	100	28/03/2022	boxcore	8.25	33.4	BE2022_08
	7	05/07/2022	Scientific diver	18.5	33.5	SiSt22-370
Summer	15	05/07/2022	Scientific diver	18.5	33.5	SiSt22-370
	25	05/07/2022	Scientific diver	18.5	33.5	SiSt22-370
	7	06/09/2022	Scientific diver	20	33.3	SiSt22-520
	15	07/09/2022	Scientific diver	20	33.3	SiSt22-520
Fall	25	08/09/2022	Scientific diver	20	33.3	SiSt22-520
	100	10/17/2022	boxcore	20	33.3	BE2022_25

Table S. 2: Field-data available to constrain model output.

Model info	Resolution	Use
Profiles: TOC, NH_3, NO_3^-	Each cm down to 12 cm max.	Used in fitting algorithm
Profiles: O_2	100 µm steps down to 0% oxygen	Not used due to uncertainty about the correspondence profile measuring setting – field situation.
Profiles: sediment porosity	Each cm	Average value used (1 measurement for all seasons / directions).
Bottom water solute concentrations		Used as parameter in model setup
Bottom water temperature	Unique to each season / distance	Used as parameter in model setup

Bottom water salinity	Unique to each season / distance	Used as parameter in model setup
Fluxes: DIC - Oxygen	For 1 season only	Not used due to uncertainty about the correspondence incubation measuring setting – field situation.

Table S. 3: Parametrization of the diagenetic model

Parameter	Description	Units	Estimated / Measured value	Range	Source
*Cflux**	Carbon deposition flux	mmol C m^{-2} d^{-1}	120	10 - 750	See table 4
*pFast**	Proportion fast-degrading carbon	-	0.74		Soetaert et al., 1996 after Westrich & Berner, 1984
w	Sediment accretion rate (solids)	m d^{-1}	2.74 10^{-6}		Diesing et al., 2021
*rFast**	Degradation rate fast-degrading carbon	d^{-1}	5.5 10^{-2}	4.87 10^{-3} – 2.74 10^{-1}	Towards upper range reported in Arndt et al. (2013). Value established by manual fitting, varies with Q_{10}.
*rSlow**	degradation rate slow-degrading carbon	d^{-1}	5.5 10^{-3}	2.74 10^{-6} – 8.7 10^{-3}	Towards upper range reported in Arndt et al. (2013). Value established by manual fitting.
Biot - Db	Bioturbation rate	cm^2 d^{-1}	5 10^{-5}	2.74 10^{-5} – 8 10^{-2}	Range from Zhang et al. (2019) - Teal et al. (2008), finetuned by data manual fitting, varies with Q_{10}.

biotdepth	Depth of mixed layer	m	$10\ 10^{-2}$	$1\ 10^{-2}$ - $1.5\ 10^{-1}$	Value varies with *k* and *Db* according to Middelburg, (2019), (See supplementary MM).
biotatt	Attenuation bioturbation profile	m	0.01		Soetaert et al. (1996)
NCrFdet	N:C ratio fast degrading carbon	molN/molC	$1.51\ 10^{-1}$		Redfield (1934)
NCrSdet	N:C ratio slow degrading carbon	molN/molC	$1.33\ 10^{-1}$		Soetaert et al. (1996)
PCrFdet	P:C ratio fast degrading carbon	molP/molC	$9.75\ 10^{-3}$		Redfield (1934)
PCrSdet	P:C ratio slow degrading carbon	molP/molC	$5\ 10^{-3}$		Soetaert et al. (1996)
O2bw	Bottom water O2 concentration	mmol m^{-3}	300		Average of field observations
NO3bw	Bottom water NO3 concentration	mmol m^{-3}	Site specific	0.3 – 13.2	Field data
NH3bw	Bottom water NH3 concentration	mmol m^{-3}	Site specific	0.8 – 25.7	Field data
ODUbw	Bottom water OD concentration	mmol m^{-3}	0		Soetaert et al. (1996)
PO4bw	Bottom water PO4 concentration	mmol m^{-3}	Site specific	0 - 0.8	Field data
DICbw	Bottom water DIC concentration	mmol m^{-3}	Site specific	$2.20\ 10^{+3}$	Field data

NH₃Ads	Constant for adsorption of NH_3 to solid fraction	-		1.3	Soetaert et al. (1996)
*rNit**	Maximum nitrification rate	d^{-1}	20	5 - 29	Fixed rate from Soetaert et al. (1996). Range from Cook et al. (2006)
ksO2nitri	Half-saturation for O2 limitation in nitrification	mmol O_2 m^{-3}	3		Soetaert et al. (1996)
rODUox	Maximum rate ODU oxidation	d^{-1}	20		Soetaert et al. (1996)
ksO2oduox	Half-saturation for O_2 limitation in ODU oxidation	mmol O_2 m^{-3}	10	1 - 20	Soetaert et al. (1996)
ksO2oxic	Half-saturation for O_2 limitation in oxic mineralization	mmol O_2 m^{-3}	3		Soetaert et al. (1996)
ksNO3denit	Half-saturation for NO_3 limitation in denitrification	mmol NO_3 m^{-3}	30		Soetaert et al. (1996)
*kinO2denit**	Half-saturation for O_2 inhibition in denitrification	mmol O_2 m^{-3}	1		Soetaert et al. (1996)
kinNO3anox	Half-saturation for NO3 inhibition in anoxic mineralization	mmol NO_3 m^{-3}	1		Soetaert et al. (1996)
kinO2anox	Half-saturation for O_2 inhibition in anoxic mineralization	mmol O_2 m^{-3}	1		Soetaert et al. (1996)

TOC0	Refractory organic carbon as % of sediment mass	%	Site specific	0.01 – 0.05	Lowest values TOC profiles
rFePdesorp	Rate of FeP desorption	d^{-1}	$1.40\ 10^{-2}$	$1.4\ 10^{-3}$ – $2.74\ 10^{-1}$	De Borger et al. (2021)
rFePadsorp	Rate of FeP adsorption	d^{-1}	$1.40\ 10^{-1}$	$1.4\ 10^{-2}$ – 2.74	De Borger et al. (2021)
rCaPprod	Rate of CaP production	d^{-1}	$2.74\ 10^{-3}$	$2.74\ 10^{-6}$ – $5.5\ 10^{-2}$	De Borger et al. (2021)
rCaPdiss	Rate of CaP dissolution	d^{-1}	2.74 10-3	$2.74\ 10^{-6}$ – $5.5\ 10^{-2}$	De Borger et al. (2021)

Table S. 4: Output of statistical analyses for seasonal and distance-related differences between measured environmental parameters.

			SS	df	F	parametric P(>F)	resampled P(>F)	Comments
Median grain size	Surface	season	12200.7	2	4.440	0.021	0.005	Non-normality detected in residual structure of initial linear model, permutation test performed.
		distance	259.1	3	0.063	0.979	0.907	
		season:distance	26628.8	6	3.230	0.015	0.009	
		Residuals	39843.6	29				
	Subsurface		SS	df	F	Pr (>F)		Comments
		season	25288	2	12.47	< 0.001		
		distance	2407	3	0.79	0.508		
		season:distance	33349	6	6.58	< 0.001		
		Residuals	30413	30				
TOC	Surface		SS	df	F	parametric P(>F)	resampled P(>F)	Comments
		season	0.0028	2	3.413	0.047	0.009	Non-normality detected in residual structure of initial linear model, permutation test performed.
		distance	0.00047	3	0.384	0.765	0.56	
		season:distance	0.00153	6	0.620	0.713	0.6	
		Residuals	0.01191	29				

			SS	df	F	parametric P(>F)	resampled P(>F)	Comments
	Subsurface	season	0.00359	2	14.949	< 0.001	< 0.001	Slight heteroscedasticity detected in residual structure of initial linear model, permutation test performed.
		distance	0.00097	3	2.695	0.064	0.027	
		season:distance	0.00214	6	2.973	0.021	0.013	
		Residuals	0.00360	30				
Chlorophyll a	Surface		SS	df	F	parametric P(>F)	resampled P(>F)	Comments
		season	3.4309	2	10.058	< 0.001	< 0.001	Normality detected in residual structure of initial linear model, permutation test performed.
		distance	0.5513	3	1.077	0.374	0.215	
		season:distance	1.9662	6	1.921	0.111	0.07	
		Residuals	4.9463	29				
	Subsurface		SS	df	F	parametric P(>F)	resampled P(>F)	Comments
		season	0.4219	2	22.442	< 0.001	< 0.001	Non-normality detected in residual structure of initial linear model, permutation test performed.
		distance	0.052	3	1.845	0.163	0.083	
		season:distance	0.5678	6	10.068	< 0.001	< 0.001	
		Residuals	0.2538	29				
Pheophorbide a	Surface		SS	df	F	parametric P(>F)	resampled P(>F)	Comments
		season	0.0089	2	8.553	< 0.001	< 0.001	Non-normality detected in residual structure of initial linear model, permutation test performed.
		distance	0.00415	3	2.657	0.067	0.034	
		season:distance	0.00746	6	2.387	0.054	0.031	
		Residuals	0.0151	29				
	Subsurface		SS	df	F	parametric P(>F)	resampled P(>F)	Comments
		season	0.00935	2	1.435	0.254	0.1	Non-normality detected in residual structure of initial linear model, permutation test performed
		distance	0.00591	3	0.605	0.617	0.417	
		season:distance	0.01036	6	0.530	0.781	0.67	
		Residuals	0.09773	30				
Pheophytin	Surface		SS	df	F	parametric P(>F)	resampled P(>F)	Comments

			SS	df	F	parametric P(>F)	resampled P(>F)	Comments
		season	0.07083	2	4.681	0.017	0.003	Non-normality detected in residual structure of initial linear model, permutation test performed.
		distance	0.00412	3	0.182	0.908	0.777	
		season:distance	0.0273	6	0.601	0.727	0.611	
		Residuals	0.21939	29				
	Subsurface		SS	df	F	parametric P(>F)	resampled P(>F)	Comments
		season	0.08712	2	0.663	0.523	0.271	Non-normality detected in residual structure of initial linear model, permutation test performed.
		distance	0.09468	3	0.480	0.699	0.503	
		season:distance	0.22307	6	0.565	0.754	0.646	
		Residuals	1.9725	30				

Table S. 5: Measured subsurface (2 cm – 12 cm, average ± SD) values for median grain size (MGS, µm), permeability (m2), total organic carbon (TOC, %), chlorophyll a (Chl a, µg g-1), pheophorbide (µg g-1), and pheophytin (µg g-1).

Season	Distance (*m*)	MGS (μm)	TOC (%)	Chl a ($\mu g\ g^{-1}$)	Pheophorbide ($\mu g\ g^{-1}$)	Pheophytin ($\mu g\ g^{-1}$)
spring	7	333 ± 58	0.08 ± 0.02	1.24 ± 1.86	0.10 ± 0.12	0.39 ± 0.67
spring	15	351 ± 34	0.05 ± 0.01	0.22 ± 0.35	0.02 ± 0.03	0.05 ± 0.11
spring	25	28 ± 16	0.08 ± 0.03	0.70 ± 0.48	0.06 ± 0.08	0.05 ± 0.03
spring	75	341 ± 23	0.04 ± 0.01	0.29 ± 0.30	0.01 ± 0.01	0.02 ± 0.02
summer	7	342 ± 2	0.07 ± 0.02	0.37 ± 0.15	0.05 ± 0.04	0.06 ± 0.03
summer	15	372 ± 26	0.04 ± 0.01	0.12 ± 0.05	0.02 ± 0.01	0.03 ± 0.02
summer	25	392 ± 61	0.05 ± 0.01	0.14 ± 0.06	0.02 ± 0.02	0.04 ± 0.02
autumn	7	350 ± 12	0.04 ± 0.01	0.11 ± 0.06	0.01 ± 0.01	0.01 ± 0.00
autumn	15	370 ± 36	0.05 ± 0.01	0.29 ± 0.16	0.02 ± 0.02	0.02 ± 0.01
autumn	25	462 ± 63	0.04 ± 0.01	0.07 ± 0.10	0.00 ± 0.01	0.01 ± 0.00
autumn	75	370 ± 37	0.03 ± 0.01	0.15 ± 0.11	0.00 ± 0.00	0.01 ± 0.00

1